Atmos. Meas. Tech., 9, 2093–2101, 2016
www.atmos-meas-tech.net/9/2093/2016/
doi:10.5194/amt-9-2093-2016

Atmospheric Measurement Techniques
Open Access
EGU

Development of automated preparation system for isotopocule analysis of N_2O in various air samples

Sakae Toyoda[1] **and Naohiro Yoshida**[1,2,3]

[1]Department of Environmental Science and Technology, Tokyo Institute of Technology, Yokohama, 226-8502, Japan
[2]Department of Environmental Chemistry and Engineering, Tokyo Institute of Technology, Yokohama, 226-8502, Japan
[3]Earth-Life Science Institute, Tokyo Institute of Technology, Tokyo, 152-8550, Japan

Correspondence to: Sakae Toyoda (toyoda.s.aa@m.titech.ac.jp)

Received: 18 January 2016 – Published in Atmos. Meas. Tech. Discuss.: 8 February 2016
Revised: 5 April 2016 – Accepted: 30 April 2016 – Published: 11 May 2016

Abstract. Nitrous oxide (N_2O), an increasingly abundant greenhouse gas in the atmosphere, is the most important stratospheric ozone-depleting gas of this century. Natural abundance ratios of isotopocules of N_2O, NNO molecules substituted with stable isotopes of nitrogen and oxygen, are a promising index of various sources or production pathways of N_2O and of its sink or decomposition pathways. Several automated methods have been reported to improve the analytical precision for the isotopocule ratio of atmospheric N_2O and to reduce the labor necessary for complicated sample preparation procedures related to mass spectrometric analysis. However, no method accommodates flask samples with limited volume or pressure. Here we present an automated preconcentration system which offers flexibility with respect to the available gas volume, pressure, and N_2O concentration. The shortest processing time for a single analysis of typical atmospheric sample is 40 min. Precision values of isotopocule ratio analysis are < 0.1 ‰ for $\delta^{15}N^{bulk}$ (average abundances of $^{14}N^{15}N^{16}O$ and $^{15}N^{14}N^{16}O$ relative to $^{14}N^{14}N^{16}O$), < 0.2 ‰ for $\delta^{18}O$ (relative abundance of $^{14}N^{14}N^{18}O$), and < 0.5 ‰ for site preference (SP; difference between relative abundance of $^{14}N^{15}N^{16}O$ and $^{15}N^{14}N^{16}O$). This precision is comparable to that of other automated systems, but better than that of our previously reported manual measurement system.

1 Introduction

Long-term monitoring of trace gases that are increasingly abundant in the atmosphere is fundamental for the analysis of the imbalance of their sources and sinks and for the prediction of future environmental change on Earth. Nitrous oxide (N_2O) is one such trace gas, with global warming potential that is 220 times as great as that of carbon dioxide (CO_2), and is the most important stratospheric ozone-depleting gas of this century (Myhre et al., 2013; Ravishankara et al., 2009). Its globally averaged concentration, given as a mole fraction, was about 324 nmol mol^{-1} (10^{-9} moles per mole of dry air) in 2011 (Hartmann et al., 2013) and increases by 0.73 nmol mol^{-1} a^{-1} (Ciais et al., 2013). Sources of N_2O include natural and agricultural soils, aqueous environments such as oceans, rivers, and lakes, industrial processes such as fossil fuel combustion, biomass burning, and animal and human wastes (Ciais et al., 2013); its major sink is photochemical decomposition in the stratosphere.

Although concentration analyses yield quantitative information related to trace gases straightforwardly, it is often difficult to differentiate the sources contributing to the increase of such gases in the atmosphere, especially for N_2O. Natural abundance ratios of stable isotopes of the elements that compose trace gas molecules have qualitative information related to the origin and production–decomposition processes of the gases because isotope ratios are generally different among different substrates. Moreover, they can change during physical, chemical, and biological processes. Regarding N_2O, measurements of the nitrogen isotope ratio ($^{15}N/^{14}N$) for the atmosphere and various sources since the 1980s have

revealed that the imbalance of isotopically light N_2O from surface sources and isotopically heavy N_2O refluxed from the stratosphere after its partial decomposition causes a progressive decrease in the $^{15}N/^{14}N$ isotope ratio of tropospheric N_2O (Ishijima et al., 2007; Röckmann et al., 2003a; Sowers et al., 2002). Furthermore, a technique developed for measuring isotopomers of N_2O ($^{14}N^{15}N^{16}O$ and $^{15}N^{14}N^{16}O$) expanded conventional isotopic analysis to isotopocule analysis by which ratios of NNO molecules substituted with stable isotopes of nitrogen or oxygen at any site relative to $^{14}N^{14}N^{16}O$ are obtained and by which production and decomposition pathways can be differentiated in greater detail (Toyoda et al., 2015 and references therein).

Compared to concentration analysis, stable isotope and isotopocule analyses require (1) larger sample amounts, (2) more time and labor to extract and purify the target compound from the sample, and (3) larger and more expensive apparatus. Although recently developed tunable diode laser absorption spectroscopy (TDLAS) relaxes some of the requirements above, and although it has some potential for on-site monitoring of stable isotope / isotopocule ratios of trace gases (Harris et al., 2014; Mohn et al., 2012; Tuzson et al., 2008), mass spectrometry combined with flask sampling still holds advantages for high-precision isotopic monitoring at polar regions or remote areas and flight observation using a balloon or an airplane because of smaller sample volume requirements.

In most currently used mass spectrometric analytical methods for N_2O isotopocules, air samples are first passed through chemical adsorbents to remove CO_2 and water vapor. Then, N_2O is concentrated on chemically inert adsorbents or inner walls of narrow tubes at liquid nitrogen temperatures. It is further purified on a capillary column of a gas chromatograph (GC) and is introduced directly into an isotope ratio monitoring mass spectrometer (IRMS). The analysis of a single sample takes 30–60 min. The precision reported in earlier studies is typically 0.1–0.5 ‰ for 1 nmol of N_2O (e.g., Toyoda et al., 2001) (See Sect. 2.4 for notation of isotopocule ratios), which is worse than the ultimate precision expected from the shot-noise limit of the IRMS (Potter et al., 2013) and which is insufficient to resolve the secular trend of atmospheric N_2O isotopocule ratios. This low precision is partly caused by incomplete separation of interfering components such as CO_2 and fluorinated hydrocarbons, or by imprecise manual handling during sample preparation.

To improve the precision of the isotopocule ratio analysis of atmospheric N_2O and to reduce the labor for complicated sample preparation procedures for mass spectrometric analysis, several automated methods have been reported. Röckmann et al. (2003b) improved the precision of fragment ion (NO^+) analysis by modifying the gas chromatographic purification of N_2O from interfering species such as halocarbons and less volatile compounds (Röckmann et al., 2003b). Röckmann and Levin (2005) and Potter et al. (2013) reported further improvement in the precision by partially or fully automating sample preparation steps and by slightly increasing the sample size.

In addition to the mass spectrometric method, an automated sample preparation system has been reported, which can be coupled to a quantum cascade laser absorption spectrometer (QCLAS) for the monitoring of atmospheric isotopocules of N_2O (Harris et al., 2014; Mohn et al., 2010). However, previously reported automated methods entail several shortcomings. For example, they are designed to measure pressurized air samples such as ambient air drawn by pumps or air collected into glass bottles or metal cylinders using pumps. For that reason, they are not applicable to samples at ambient or subambient pressure.

Here we present an automated preconcentration system that offers enhanced flexibility in terms of sample gas pressure and N_2O concentration. The novel system encloses a vacuum line and a computer program that controls valves to inject samples of a designated amount.

2 Preparation system

The preparation system developed in this study consists of a sample injection unit, cryogenic concentration unit, purification unit, and cryofocusing unit (Fig. 1). It is placed in a steel rack (60 cm width, 80 cm depth, 150 cm height) with wheels attached, and is connected to a gas chromatograph–isotope ratio monitoring mass spectrometer (GC-IRMS). Details of each unit are presented below.

2.1 Sample injection unit

This unit consists of a multi-position six-port switching valve (E4SD6MWE; Valco Instruments Co. Inc., Houston, TX, SV1 in Fig. 1) equipped with an electric actuator, air-actuated diaphragm shut-off valves (FPR-ND-71-6.35-2; Fujikin, Osaka, Japan, V1−V5 in Fig. 1), a pressure gauge (VSHT21; Valcom Co. Ltd., Toyonaka, Japan, PG1 in Fig. 1), a capacitance manometer (Barocel Model 600; BOC Edwards, Wilmington, MA, PG2 in Fig. 1), a Pirani vacuum gauge (GP-2A; ULVAC, Inc., Chigasaki, Japan, VG in Fig. 1), a vacuum pump system (turbo drag pump TMH 071 P and diaphragm pump MVP 015-2 with a controller; Pfeiffer Vacuum GmbH, Asslar, Germany, VP in Fig. 1), three custom-made glass bottles, and stainless steel (ss) tubing.

A sample flask (made of either glass or ss) or a gas cylinder is manually connected to one of the switching valve ports with an ss connector (Cajon Ultra-Torr or Swagelok; Swagelok Company, Solon, OH). The tubing between the diaphragm valve (V1, V2, or V3) and the flask/cylinder valve is evacuated by manually operating the valves and vacuum pump via control software (see below). Then, all the diaphragm valves are closed, the flask valve is opened by hand, and a computer program for sample preparation (see Sect. 2.5) is started.

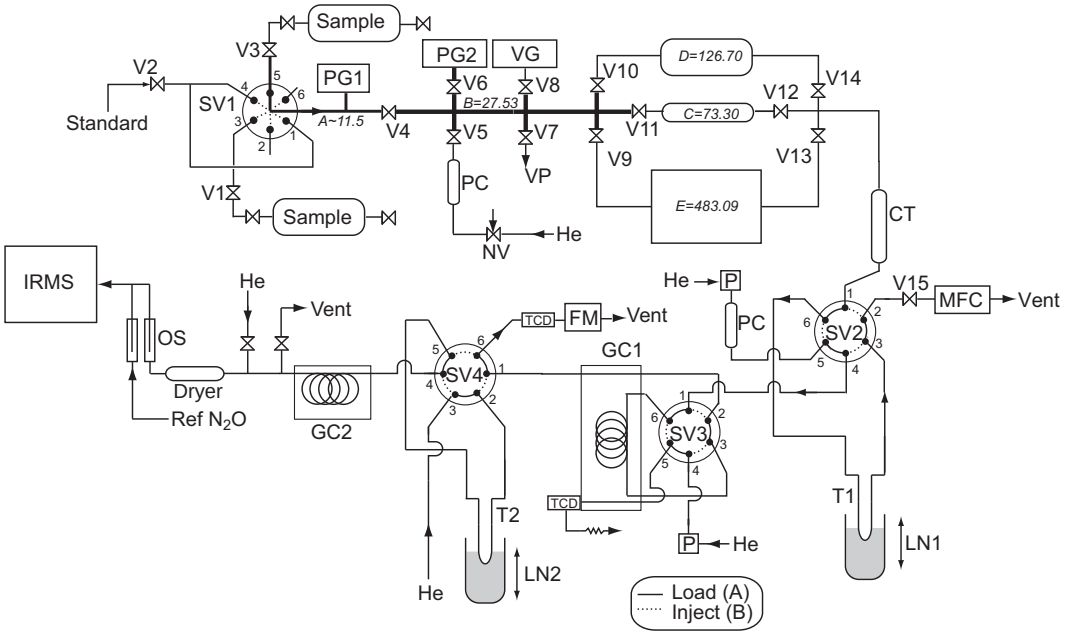

Figure 1. Schematic portraying the sample preparation system developed in this study: CT, chemical trap; FM, flow monitor; GC, gas chromatograph; IRMS, isotope ratio mass spectrometer; LN, liquid nitrogen; MFC, mass flow controller; NV, needle valve; OS, open split interface; P, pressure regulator; PC, purification column; PG, pressure gauge; SV, electrically actuated switching valve; T, trap; V, air-actuated diaphragm valve; VG, vacuum gauge; VP, vacuum pump. A–E denote parts of the vacuum line or glass bottles that are used to expand the sample, the volume (cm^3) of which is also shown.

First, sample gas pressure in the flask is measured using the pressure gauge by expanding the sample gas into the vacuum line until V4. Based on the pressure and the volume of the flask and the sample size to be injected, the "sample expanding option" and final pressure of the sample injected into the vacuum line is calculated. Seven options exist for sample expansion into the calibrated volume in the vacuum line from 100 cm^3 (option no. 1) to 510 cm^3 (option no. 7). This expansion is realized by a combination of the three glass bottles (C, D, and E in Fig. 1) with different volumes.

Next, an aliquot of the sample in the flask is expanded by sequential open–close operation of diaphragm valves. The pressure is monitored using the manometer. When the pressure agrees with the precalculated value within ±5 %, either V1 or V3 (when sample is analyzed, Fig. 1) or V2 (when standard gas is analyzed) and V4 are closed, the pressure is recorded, and the injected sample amount is calculated.

2.2 Concentration unit

This unit consists of a chemical trap (CT in Fig. 1), an electrically actuated two-position six-port switching valve (E4C6UWE; Valco Instruments Co. Inc., Houston, TX, SV2 in Fig. 1), a U-shaped concentration trap (T1 in Fig. 1), and a mass flow controller (SEC-E40; Horiba Stec Co. Ltd., Kyoto, Japan, MFC in Fig. 1). The chemical trap is a glass tube (9 mm outer diameter (o.d.), 20 cm long) packed with $Mg(ClO_4)_2$ (8–24 mesh; Wako Pure Chemical Industries Ltd., Osaka, Japan), NaOH on support (Ascarite, 20–30 mesh; Thomas Scientific), and $Mg(ClO_4)_2$ (20–48 mesh) in series with approximately equal length. The T1 is an ss tube (1/4 inch o.d., 30 cm long) packed with glass beads (Flusin GH 60–80 mesh; GL Sciences Inc., Tokyo, Japan).

First, the concentration trap is purged with ultra-pure He (> 99.9999 %, Japan Air Gases Ltd., Tokyo, Japan) at 100 $cm^3\,min^{-1}$ for > 10 s by switching SV2 to the "inject" position. The He is purified in advance through a column packed with molecular sieves 5A, active charcoal, and molecular sieves 13X in series (PC in Fig. 1). Next, SV2 is switched to the "load" position and the trap is cooled with liquid nitrogen in an ss dewar which is driven up and down by a custom-made air-actuated stage and which is filled with liquid nitrogen from an automatic liquid nitrogen supply system (Koshin Ltd., Tokyo, Japan). Then V5, V15, and valves relevant to the sample injection option (V9–V14) are opened. The sample gas in the calibrated volume is transferred to the concentration trap through the chemical trap by He carrier gas at 30 $cm^3\,min^{-1}$. The He is purified in a similar manner to that described above. When more than two glass bottles are filled with the sample gas, the transfer is conducted sequentially. The transfer time is set so that the total volume of He which flows through the bottle is twice the bottle volume.

2.3 Purification and cryofocusing unit

This unit consists of two electrically actuated two-position six-port switching valves (SV3 and SV4 in Fig. 1, E4C6UWE; Valco Instruments Co. Inc., Houston, TX), a gas chromatograph (GC-8AIT; Shimadzu Corp., Kyoto, Japan. GC1 in Fig. 1) equipped with a thermal conductivity detector (TCD), and a U-shaped cryofocusing trap (T2 in Fig. 1). The GC column is an ss tube (4 mm o.d., 3 m length) packed with Porapak Q (80–100 mesh; Waters Corp., MA). It is kept at 60 °C. The cryofocusing trap is an ss tube (1/16 inch o.d., 70 cm long) with no packing material.

Initially, SV3 and SV4 are set to the load position. After the sample concentration step is completed, SV2 is switched to the inject position. The concentration trap is heated to 70 °C by lowering the liquid nitrogen dewar and turning on a sheathed electric heater attached to the trap. The concentrated trace gases are transferred to the GC column with purified He at 20 $cm^3\,min^{-1}$. When 2 min have passed after the GC injection, the cryofocusing trap is cooled with liquid nitrogen by moving up another ss dewar. Three minutes later, SV4 is switched to the inject position. Purified N_2O from the GC is focused on the trap for 2 min.

2.4 Injection to GC-IRMS

After the cryofocusing step is completed, SV4 is switched to the load position, the liquid nitrogen dewar is moved down, and the cryofocus trap is heated to 70 °C similarly, as in the case of the concentration trap. The N_2O is injected into another GC (GC6890; Agilent Technologies Inc., Santa Clara, CA, GC2 in Fig. 1) with He (2 $cm^3\,min^{-1}$). It is further purified with the GS Carbon PLOT column (0.32 mm inner diameter (i.d.), 3 µm film thickness, 30 m; Agilent Technologies Inc.) maintained at 35 °C. The purified N_2O is finally injected into an IRMS (MAT252; Thermo Fisher Scientific K.K., Yokohama, Japan) via an interface that includes a gas dryer with a permeation tube and two open split interfaces for the sample and reference gas (GC-combustion interface; Thermo Fisher Scientific K.K., slightly modified).

Mass spectrometric analysis of N_2O isotopocules is conducted as described elsewhere (Toyoda and Yoshida, 1999; Toyoda et al., 2015). Briefly, molecular (N_2O^+) and fragment (NO^+) ions of N_2O are analyzed in independent runs. Solving the following equations and applying correction for the rearrangement or scrambling reactions during fragmentation, the isotopocule ratios are obtained as delta values.

$$^{45}R = {}^{15}R^{\alpha} + {}^{15}R^{\beta} + {}^{17}R \quad (1)$$

$$^{46}R = {}^{18}R + ({}^{15}R^{\alpha} + {}^{15}R^{\beta})\,{}^{17}R + {}^{15}R^{\alpha}\,{}^{15}R^{\beta} \quad (2)$$

$$^{31}R = {}^{15}R^{\alpha} + {}^{17}R \quad (3)$$

$$^{17}R = A(^{18}R)^{\gamma} \quad (4)$$

$$\delta^{15}N^{i} = {}^{15}R^{i}_{\text{sample}} / {}^{15}R^{i}_{\text{standard}} - 1 \; (i = \alpha, \beta, \text{ or bulk}) \quad (5)$$

$$\delta^{18}O = {}^{18}R_{\text{sample}} / {}^{18}R_{\text{standard}} - 1 \quad (6)$$

$$SP = \delta^{15}N^{\alpha} - \delta^{15}N^{\beta} \quad (7)$$

In Eqs. (1)–(6), ^{45}R and ^{46}R respectively denote the measured ion-beam intensity ratios of m/z 45/44 and 46/44 in molecular ion analysis; ^{31}R shows a 31/30 ratio by fragment ion analysis; $^{15}R^{\alpha}$, $^{15}R^{\beta}$, ^{17}R, and ^{18}R respectively denote the abundance of ions $^{14}N^{15}N^{16}O^+$, $^{15}N^{14}N^{16}O^+$, $^{14}N^{14}N^{17}O^+$, and $^{14}N^{14}N^{18}O^+$ relative to $^{14}N^{14}N^{16}O^+$. In Eq. (4), $A = 0.00937035$ and $\gamma = 0.516$ (Kaiser et al., 2003). In Eq. (5), $\delta^{15}N^{\text{bulk}}$ denotes the average isotope ratios for $^{15}N/^{14}N$. The subscripts sample and standard respectively denote the isotope ratios for the sample and the standard. SP denotes site preference. International standards for N and O isotope ratios are atmospheric N_2 and Vienna Standard Mean Ocean Water (VSMOW), respectively.

2.5 Operation by PC software

A personal computer (NI PXI-1042Q with a controller NI PXI-8196 and I/O boards NI PXI-6221, NI PXI-4351, NI PXI-8421, and NI PXI-6514; National Instruments Corp., Austin, TX) and programming software (LabVIEW Ver. 8.2; National Instruments Corp., Austin, TX) were used to activate the solenoid valves that regulate compressed air for air-actuated shut-off valves and the air-actuated up–down stages, the multi/two-position switching valves, the vacuum pump system, the automatic liquid nitrogen supply system, and the temperature controller for the heaters. The PC also received analogue data from the pressure and vacuum gauges and from the manometer, received the TCD signal, and synchronized the GC-IRMS data acquisition with the end of the sample preparation procedure. The timing of each regulation function is presented in Fig. 2.

The program developed in this study includes a special algorithm to adapt the sampling procedure to the prevailing sample pressure and N_2O concentration. As described briefly in Sect. 2.1, it has a user interface to obtain information related to the sample: the flask volume and the sample size to be injected. When the actual sample gas pressure is measured and obtained, it automatically determines the optimal procedure for sample injection. Figure 3 shows a flow chart for the algorithm.

3 Results and discussion

3.1 Sample injection to the system

The time required for sample injection depends on the sample expanding option (see Sect. 2.1). It takes about 5 min when a 300 cm^3 aliquot of air, which contains ca. 4 nmol of N_2O in the case of ambient air (ca. 320 $nmol\,mol^{-1}$), is injected from a 1 L flask pressurized to about 2.5 atm (option no. 7). When the flask volume or inner pressure is lower, more time is needed because the number of repetitive sample

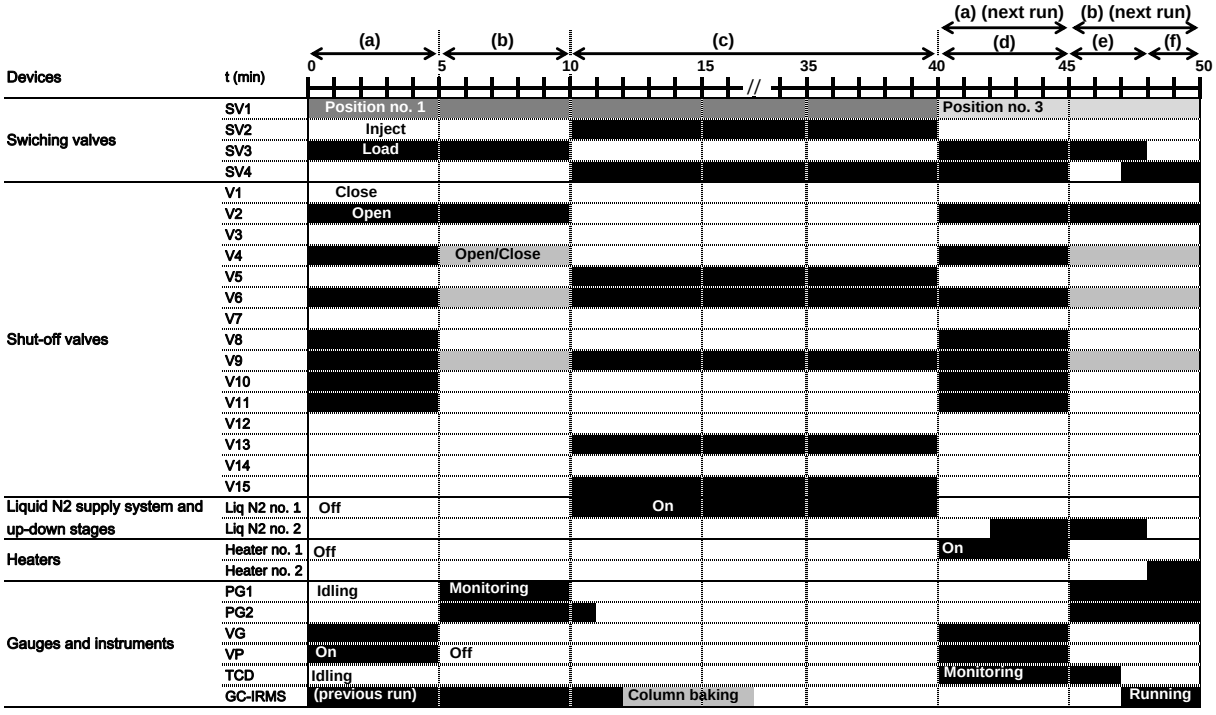

Figure 2. Time sequence of the sample preparation procedure. Horizontal arrows on the top indicate the periods for evacuation of the inlet line **(a)**, sample injection **(b)**, cryogenic concentration of N_2O on T1 **(c)**, purification of N_2O by GC1 **(d)**, cryofocusing of N_2O on T2 **(e)**, and injection of N_2O into GC2 **(f)**. See also Fig. 1.

diffusion steps increases and one valve was operated 5 s after actuating another valve to equilibrate the pressure in the inlet line and to avoid potential fractionation of isotopocules.

When a smaller sample volume with high N_2O concentration is measured, sample injection is completed in a minute or less. However, the performance of quantitative sample injection becomes poor for samples with more than 10 µmol mol^{-1} N_2O because the system cannot fully adjust the introduction of a small amount of sample ($< 10\,cm^3$). Moreover, the relative error of the pressure measurement increases for low pressure. Such highly concentrated samples are better introduced after dilution with N_2 or He. Modification of one glass bottle (e.g., bottle C) to enable manual injection with a microsyringe is also possible.

3.2 Concentration, purification, and cryofocusing of N_2O

During cryogenic concentration of N_2O, the flow rate and flowing time of the He carrier gas should be optimized carefully to ensure quantitative recovery of N_2O and thus also minimize contamination of subsequent analyses (blank values). Our preliminary tests showed that each glass bottle (C, D, or E) is purged completely when the total volume of He is more than twice the bottle volume. This result indicates that laminar flow is predominant in the bottle. Turbulent flow, which is expected to cause exponential dilution and to result in the consumption of a larger amount of He to sweep out the initial sample gas, is negligible.

The main purpose of the purification step is separation of N_2O from CO_2 and compounds that are less volatile than N_2O. CO_2 is 1000 times more abundant than N_2O in ambient air samples. Its isotopocules have the same mass as those of N_2O. Therefore, it often interferes with mass spectrometric analysis of N_2O molecular ions. We tested two column packing materials for this purpose: Porapak Q and silica gel (dimension of the column was identical to that of Porapak Q, 60–80 mesh; GL Sciences Inc., Tokyo, Japan). Although silica gel has the unique property of eluting N_2O before CO_2, their separation took longer than in Porapak Q. The separation was not complete, even at 50 °C with the flow rate of 15–50 cm^3 min^{-1}. We also strove to separate CO_2 and N_2O without using chemical adsorbents, which revealed a condition under which CO_2 and N_2O are separated almost completely in preliminary experiments using a thermal conductivity detector and a mixture of CO_2 and N_2O in N_2 bath gas (mixing ratios of CO_2 and N_2O were ca. 250 µmol mol^{-1}). However, a small CO_2 peak was observed on the m/z 44 chromatogram after separation by the second GC. Mass ratios ^{45}R and ^{46}R showed dependence on the area of CO_2 peak, which indicates that separation on the first column was insufficient for precise isotopocule ratio analysis of N_2O. Therefore, we inserted the chemical CO_2 trap before cryogenic concentration. Volatile compounds such as halocarbons and hydrocarbons

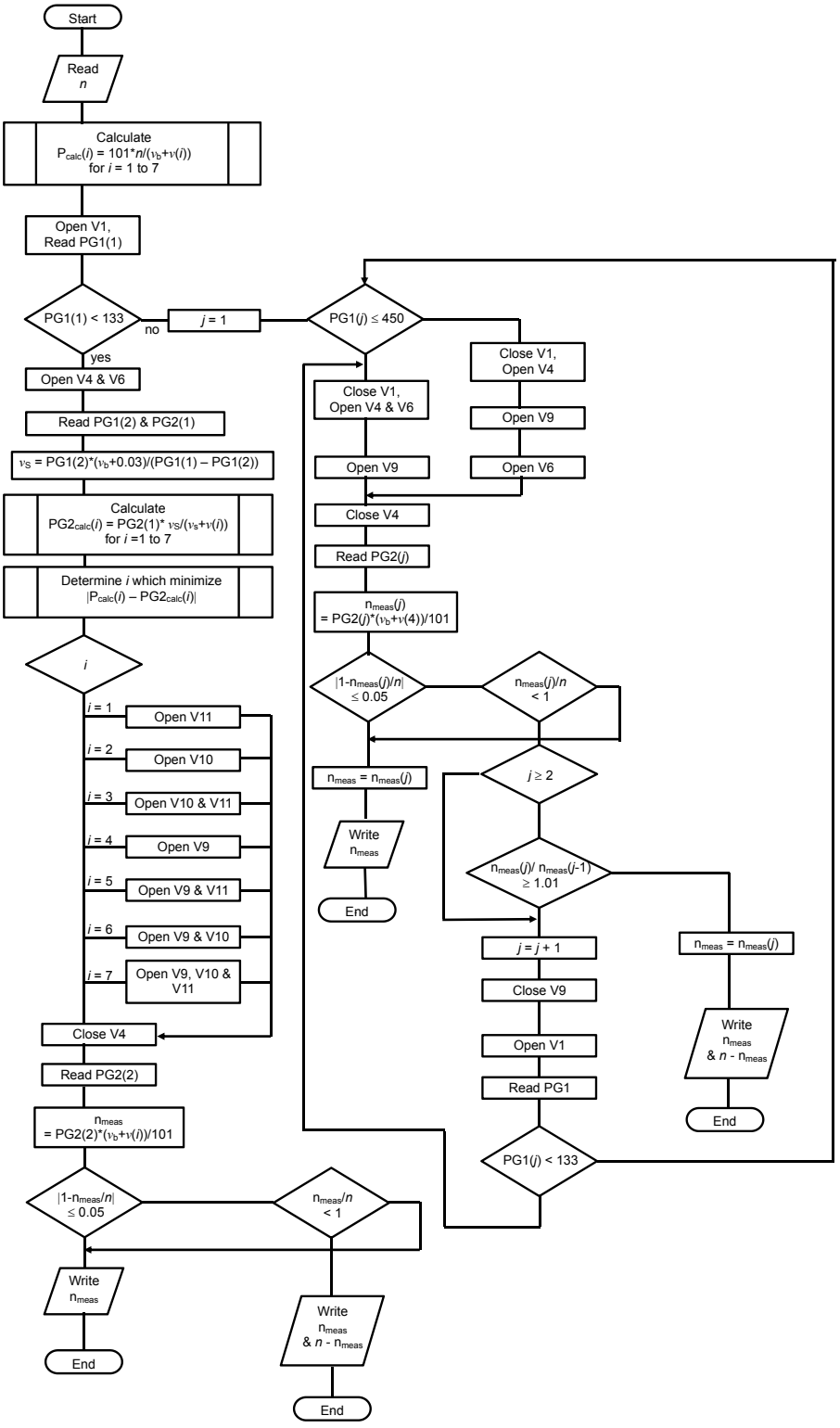

Figure 3. Flow chart of the algorithm for sample injection. n denotes the sample size in cubic centimeters at 25 °C and 1 atm. n_{meas} or $n_{\mathrm{meas}}(j)$ is the actual sample size calculated from measured pressure. v_{b} is the partial volume (cm^3) of the vacuum line indicated by B in Fig. 1. $v(i)$ is the calibrated volume that corresponds to the sample expanding option i. v_{S} is sum of the volume of sample flask and partial volume A. PG1(j) and PG2(j) are outputs of pressure gauges 1 and 2 (in kPa) (Fig. 1). $\mathrm{P_{calc}}(i)$ and $\mathrm{PG2_{calc}}(i)$ are calculated pressures that correspond to the sample expanding option i.

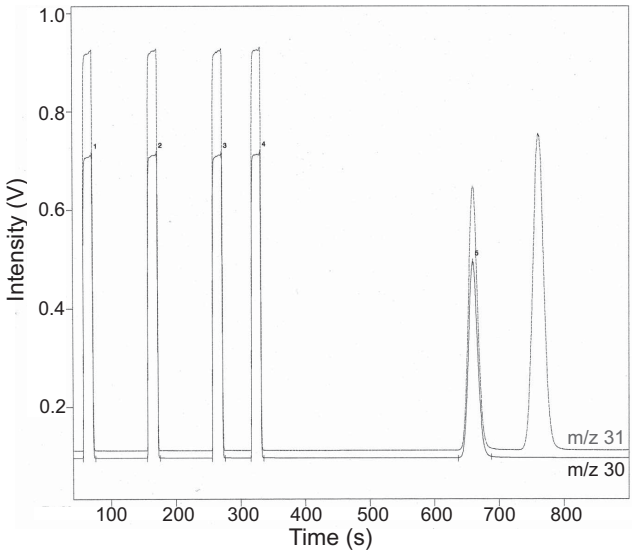

Figure 4. Typical chromatogram of background air sample obtained in a fragment-ion (NO^+) monitoring run. The x axis shows elapsed time after the start of heating of the cryofocusing trap. After the peaks of reference N_2O injected from GC-IRMS interface (no. 1–no. 4), sample N_2O peak appears (no. 5). The peak elution about 100 s later is only detected on m/z 31 trace and is CF^+ derived from a fluorinated carbon species.

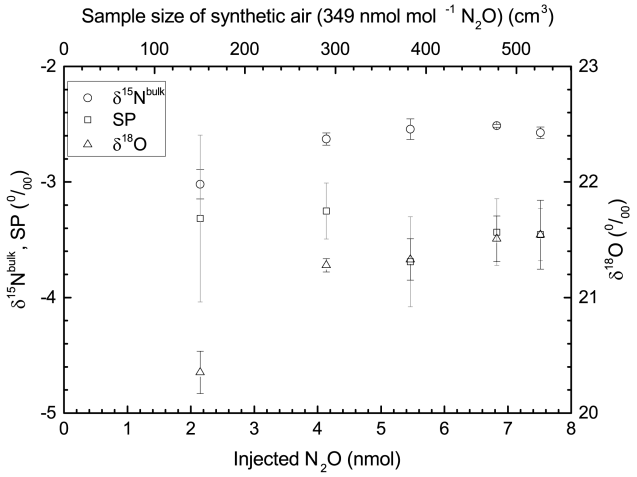

Figure 5. Precision of isotopocule ratio measurements as a function of sample size.

have longer retention time than that of N_2O on columns typically used for N_2O analysis. Some of them are known to hamper the chromatography of successive runs caused by their very slow elution (Röckmann et al., 2003b). Similar to previous studies, such compounds were prevented from being transferred to the next step and were backflushed to vent by switching the flow path in the present system.

The cryofocusing step was necessary to inject the N_2O purified in the high-flow system to the low-flow capillary GC-IRMS system. To achieve a quantitative N_2O recovery, the timing of the cryofocusing step was optimized to trap the eluent from the first column only while N_2O was released.

3.3 Optimization of GC-IRMS analysis and measurement precision

We tested two fused-silica capillary columns for the separation of N_2O from other constituents in the second GC, a porous polymer PLOT column (HP PLOT Q, 0.32 mm i.d., 20 µm film thickness, 30 m; Agilent Technologies Inc.) and a PLOT column with a monolithic carbon layer (GS Carbon PLOT). The latter column was found to have benefits for the separation of CO_2, N_2O, and other interfering compounds such as fluorinated hydrocarbons (Fig. 4). A shortcoming was that the retention time of N_2O at the optimized condition became longer than that obtained with the porous polymer column, which was used in previous studies (Potter et al., 2013; Röckmann et al., 2003b).

The degree of precision of the measurements was evaluated with the standard deviation of repeated analyses ($n = 3$) of synthetic air (349 nmol mol^{-1} N_2O) pressurized in an aluminum cylinder that had been calibrated against the international isotopic standard and which was used as a working standard (Toyoda et al., 2013). As presented in Fig. 5, precision of $\delta^{15}N^{bulk}$, $\delta^{18}O$, and SP values measured on a single day are typically better than 0.1, 0.2, and 0.5 ‰, respectively, when more than 4 nmol (which corresponds to about 300 cm^3 of the synthetic air) of N_2O is injected. The peak area of major ions m/z 44 and 30 showed good linearity with respect to the sample size (data not shown). The N_2O concentration was obtained by comparison of the peak area normalized to the specific sample size between the sample and the laboratory standard. The resulting precision of the concentration measurement is better than 0.5 % (coefficient of variation, $n = 3$). In addition, measured isotopocule ratios are independent of the sample size of 4–8 nmol. Results show that routine analyses of atmospheric air samples can be conducted with samples of 320 cm^3 so that measurements of each sample are sandwiched by those of the working standard (Table 2).

The performance of the developed system is presented along with that of previous works in Table 1. The precision and required sample size of this work is comparable to that of similar automated GC-IRMS systems. It takes 40 min for a single run, which means that a total of 80 min is necessary to obtain a single set of $\delta^{15}N^{bulk}$, $\delta^{18}O$, and SP on some mass spectrometers that are incapable of simultaneous monitoring of five ions (m/z 44, 45, 46, 30, and 31). This might be a shortcoming of the present system, but it presents advantages in terms of flexibility of the sample pressure and sample size.

Table 1. Comparison of the analytical precision obtained in this study and those values reported in the literature.

Reference	Sample size	Precision (1 standard deviation) (‰)					Analytical	Notes
	(cm^3 of ambient air)	$\delta^{15}N^{bulk}$	$\delta^{15}N^{\alpha}$	$\delta^{15}N^{\beta}$	SP	$\delta^{18}O$	time (min)	
Toyoda et al. (2001)	100	0.1–0.5	0.5–1	0.5–1	1–2	0.1–0.5	25	Manual system with MAT252 ($n = 3$)
Toyoda et al. (2013)	300	0.1	0.3	0.4	0.6	0.3	35	Manual system with MAT252 ($n = 3$)
Röckmann et al. (2003b)	125–167	0.1	0.3[a]	0.4[b]	0.6[b]	0.2	NA[c]	Automated system with Delta Plus XL ($n = 5$–20)
Röckmann and Levin (2005)	333	0.06	NA	NA	NA	0.09	20	Automated system with Delta Plus XP
Mohn et al. (2010)	10 000	NA	0.24	0.17	0.29[b]	NA	ca. 30	Automated system with quantum cascade laser ($n = 136$)
Wolf et al. (2015)	8000	0.12	0.20	0.12	0.22	0.10	ca. 30	Fully automated system with QCLAS ($n = 331$)
Potter et al. (2013)	420	0.05	0.11	0.14	0.21	0.10	NA	Fully automated system with MAT253 ($n = 3$–5)
This work	320	0.09	0.19	0.30	0.45	0.23	40	Fully automated system with MAT252 ($n = 3$)

[a] Obtained with 420 cm^3 air; [b] estimated from the reported precision for $\delta^{15}N^{\alpha}$, $\delta^{15}N^{\beta}$, or $\delta^{15}N^{bulk}$; [c] not available or not described.

Table 2. Example of measurement results conducted on a single day.

Measurement no.	Sample	$\delta^{15}N^{bulk}$	$\delta^{15}N^{\alpha}$	$\delta^{15}N^{\beta}$	$\delta^{18}O$	SP
1, 2	S	−2.69	−4.17	−1.20	21.22	−2.97
3, 4	X1	6.58	17.18	−4.02	43.05	21.20
5, 6	X1	6.80	16.63	−3.04	43.86	19.68
7, 8	S	−2.62	−4.16	−1.08	21.34	−3.08
9, 10	X2	7.71	18.51	−3.09	44.54	21.61
11, 12	X2	7.96	18.50	−2.59	44.45	21.09
13, 14	S	−2.58	−4.43	−0.73	21.28	−3.70
15, 16	X3	6.02	15.22	−3.17	43.15	18.39
17, 18	X3	6.18	16.20	−3.85	43.68	20.05
Average	S	−2.63	−4.25	−1.00	21.28	−3.25
SD	($n = 3$)	0.05	0.15	0.25	0.06	0.39
	X1	6.69	16.91	−3.53	43.46	20.44
	($n = 2$)[a]	0.11	0.28	0.49	0.41	0.76
	X2	7.83	18.51	−2.84	44.49	21.35
	($n = 2$)[a]	0.12	0.01	0.25	0.05	0.26
	X3	6.10	15.71	−3.51	43.41	19.22
	($n = 2$)[a]	0.08	0.49	0.34	0.27	0.83

[a] Difference/2 is shown.

4 Conclusions

A fully automated sample preparation system was developed for the measurement of concentrations and isotopocule ratios of N_2O in both pressurized and subatmospheric pressure samples. An ambient atmospheric sample of 320 cm^3 can be analyzed in 40 min with a precision of < 0.5 % (coefficient of variation) for concentration, < 0.1 ‰ (1 standard deviation) for $\delta^{15}N^{bulk}$, < 0.2 ‰ for $\delta^{18}O$, and < 0.5 ‰ for ^{15}N site preference (SP). The system, not being limited to use for mass spectrometric analysis, can also be applied to concentration or isotopic analyses of other trace gases such as CO_2 and CH_4 by replacing the chemical trap, GC columns, and cryogenic concentration/focusing traps and by re-optimizing the temperature, flow rate, and flow switch conditions.

Unlike previously reported systems, this system enables analysis of grab-sampled air samples that are collected into a pre-evacuated container at atmospheric pressure. This capability is particularly valuable when compressors or pumps cannot be used for sampling because of logistic reasons such as electric power or weight.

Acknowledgements. The authors thank N. Kuroki and Y. Watanabe for their assistance in the developing and optimizing of the system. This work was conducted as part of the "Studies on greenhouse gas cycles in the Arctic and their responses to climate change" under the GRENE Arctic Climate Change Research Project, and also financially supported by JSPS KAKENHI, grant numbers 17GS0203 and 23224013.

Edited by: B. Buchmann

References

Ciais, P., Sabine, C., Bala, G., Bopp, L., Brovkin, V., Canadell, J., Chhabra, A., DeFries, R., Galloway, J., Heimann, M., Jones, C., Quéré, C. L., Myneni, R. B., Piao, S., and Thornton, P.: Carbon and other biogeochemical cycles, in: Climate Change 2013: The Physical Science Basis. Contribution of Working Group I to the Fifth Assessment Report of the Intergovernmental Panel on Climate Change, edited by: Stocker, T. F., Qin, D., Plattner, G.-K., Tignor, M., Allen, S. K., Boschung, J., Nauels, A., Xia, Y., Bex, V., and Midgley, P. M., Cambridge University Press, Cambridge, UK and New York, NY, USA, 465–570, 2013.

Harris, E., Nelson, D. D., Olszewski, W., Zahniser, M., Potter, K. E., McManus, B. J., Whitehill, A., Prinn, R. G., and Ono, S.: Development of a spectroscopic technique for continuous online monitoring of oxygen and site-specific nitrogen isotopic composition of atmospheric nitrous oxide, Anal. Chem., 86, 1726–1734, 2014.

Hartmann, D. L., Tank, A. M. G. K ., Rusticucci, M., Alexander, L. V., Brönnimann, S., Charabi, Y., Dentener, F. J., Dlugokencky, E. J., Easterling, D. R., Kaplan, A., Soden, B. J., Thorne, P. W., Wild, M., and Zhai, P. M.Observations: Atmosphere and Surface, in: Climate Change 2013: The Physical Science Basis. Contribution of Working Group I to the Fifth Assessment Report of the Intergovernmental Panel on Climate Change, edited by: Stocker, T. F., Qin, D., Plattner, G.-K., Tignor, M., Allen, S. K., Boschung, J., Nauels, A., Xia, Y., Bex, V., and Midgley, P. M., Cambridge University Press, Cambridge, UK and New York, NY, USA, 159–254, 2013.

Ishijima, K., Sugawara, S., Kawamura, K., Hashida, G., Morimoto, S., Murayama, S., Aoki, S., and Nakazawa, T.: Temporal variations of the atmospheric nitrous oxide concentration and its $\delta^{15}N$ and $\delta^{18}O$ for the latter half of the 20th century reconstructed from firn air analyses, J. Geophys. Res.-Atmos., 112, D03305, doi:10.1029/2006JD007208, 2007.

Kaiser, J., Röckmann, T., and Brenninkmeijer, C. A. M.: Complete and accurate mass spectrometric isotope analysis of tropospheric nitrous oxide, J. Geophys. Res, 108, 4476, doi:10.1029/2003JD003613, 2003.

Mohn, J., Guggenheim, C., Tuzson, B., Vollmer, M. K., Toyoda, S., Yoshida, N., and Emmenegger, L.: A liquid nitrogen-free preconcentration unit for measurements of ambient N_2O isotopomers by QCLAS, Atmos. Meas. Tech., 3, 609–618, doi:10.5194/amt-3-609-2010, 2010.

Mohn, J., Tuzson, B., Manninen, A., Yoshida, N., Toyoda, S., Brand, W. A., and Emmenegger, L.: Site selective real-time measurements of atmospheric N_2O isotopomers by laser spectroscopy, Atmos. Meas. Tech., 5, 1601–1609, doi:10.5194/amt-5-1601-2012, 2012.

Myhre, G., Shindell, D., Bréon, F.-M., Collins, W., Fuglestvedt, J., Huang, J., Koch, D., Lamarque, J.-F., Lee, D., Mendoza, B., Nakajima, T., Robock, A., Stephens, G., Takemura, T., and Zhang, H.: Anthropogenic and Natural Radiative Forcing, in: Climate Change 2013: The Physical Science Basis. Contribution of Working Group I to the Fifth Assessment Report of the Intergovernmental Panel on Climate Change, edited by: Stocker, T. F., Qin, D., Plattner, G.-K., Tignor, M., Allen, S. K., Boschung, J., Nauels, A., Xia, Y., Bex, V., and Midgley, P. M., Cambridge University Press, Cambridge, UK and New York, NY, USA, 659–740, 2013.

Potter, K. E., Ono, S., and Prinn, R. G.: Fully automated, high-precision instrumentation for the isotopic analysis of tropospheric N_2O using continuous flow isotope ratio mass spectrometry, Rapid Commun. Mass Sp., 27, 1723–1738, 2013.

Ravishankara, A. R., Daniel, J. S., and Portmann, R. W.: Nitrous oxide (N_2O): The dominant ozone-depleting substance emitted in the 21st century, Science, 326, 123–125, 2009.

Röckmann, T. and Levin, I.: High-precision determination of the changing isotopic composition of atmospheric N_2O from 1990 to 2002, J. Geophys. Res., 110, D21304, doi:10.1029/2005JD006066, 2005.

Röckmann, T., Kaiser, J., and Brenninkmeijer, C. A. M.: The isotopic fingerprint of the pre-industrial and the anthropogenic N_2O source, Atmos. Chem. Phys., 3, 315–323, doi:10.5194/acp-3-315-2003, 2003a.

Röckmann, T., Kaiser, J., Brenninkmeijer, C. A. M., and Brand, W. A.: Gas chromatography/isotope-ratio mass spectrometry method for high-precision position-dependent ^{15}N and ^{18}O measurements of atmospheric nitrous oxide, Rapid Commun. Mass Sp., 17, 1897–1908, 2003b.

Sowers, T., Rodebaugh, A., Yoshida, N., and Toyoda, S.: Extending records of the isotopic composition of the atmospheric N_2O back to 1800 A.D. from air trapped in snow at the South Pole and the Greenland Ice Sheet Project II ice core, Global Biogeochem. Cy., 16, 1129, doi:10.1029/2002GB001911, 2002.

Toyoda, S. and Yoshida, N.: Determination of nitrogen isotopomers of nitrous oxide on a modified isotope ratio mass spectrometer, Anal. Chem., 71, 4711–4718, 1999.

Toyoda, S., Yoshida, N., Urabe, T., Aoki, S., Nakazawa, T., Sugawara, S., and Honda, H.: Fractionation of N_2O isotopomers in the stratosphere, J. Geophys. Res., 106, 7515–7522, 2001.

Toyoda, S., Kuroki, N., Yoshida, N., Ishijima, K., Tohjima, Y., and Machida, T.: Decadal time series of tropospheric abundance of N_2O isotopomers and isotopologues in the Northern Hemisphere obtained by the long-term observation at Hateruma Island, Japan, J. Geophys. Res., 118, 3369–3381, 2013.

Toyoda, S., Yoshida, N., and Koba, K. Isotopocule analysis of biologically produced nitrous oxide in various environments, Mass Spectrom, Rev., doi:10.1002/mas.21459, 2015.

Tuzson, B., Mohn, J., Zeeman, M. J., Werner, R. A., Eugster, W., Zahniser, M. S., Nelson, D. D., McManus, J. B., and Emmenegger, L. High precision and continuous field measurements of δ13C and δ18O in carbon dioxide with a cryogen-free QCLAS, Appl. Phys. B, 92, 451–458, 2008.

Wolf, B., Merbold, L., Decock, C., Tuzson, B., Harris, E., Six, J., Emmenegger, L., and Mohn, J.: First on-line isotopic characterization of N_2O above intensively managed grassland, Biogeosciences, 12, 2517–2531, doi:10.5194/bg-12-2517-2015, 2015.